

A Methodology for the Diagnostic of Aircraft Engine Based on Indicators Aggregation

Tsirizo Rabenoro^{1*}, Jérôme Lacaille¹, Marie Cottrell², and Fabrice Rossi²

¹ Snecma, Groupe Safran,
77550 Moissy Cramayel, France

² SAMM (EA 4543), Université Paris 1,
90, rue de Tolbiac, 75634 Paris Cedex 13, France
{tsirizo.rabenoro, jerome.lacaille}@snecma.fr
{marie.cottrell, fabrice.rossi}@univ-paris1.fr

Abstract. Aircraft engine manufacturers collect large amount of engine related data during flights. These data are used to detect anomalies in the engines in order to help companies optimize their maintenance costs. This article introduces and studies a generic methodology that allows one to build automatic early signs of anomaly detection in a way that is understandable by human operators who make the final maintenance decision. The main idea of the method is to generate a very large number of binary indicators based on parametric anomaly scores designed by experts, complemented by simple aggregations of those scores. The best indicators are selected via a classical forward scheme, leading to a much reduced number of indicators that are tuned to a data set. We illustrate the interest of the method on simulated data which contain realistic early signs of anomalies.

Keywords: Health Monitoring, Turbofan, Fusion, Anomaly Detection

1 Introduction

Aircraft engines are generally made extremely reliable by their conception process and thus have low rate of operational events. For example, in 2013, the CFM56-7B engine, produced jointly by Snecma and GE aviation, has a rate of in flight shut down (IFSD) is 0.02 (per 1000 Engine Flight Hour) and a rate of aborted take-off (ATO) is 0.005 (per 1000 departures). This dispatch availability of nearly 100 % (99.962 % in 2013) is obtained also via regular maintenance operations but also via engine health monitoring (see also e.g. [15] for an external evaluation).

This monitoring is based, among other, on data transmitted by satellites³ between aircraft and ground stations. Typical transmitted messages include engine

^{*} This study is supported by a grant from Snecma, Safran Group, one of the world's leading manufacturers of aircraft and rocket engines, see <http://www.snecma.com/> for details.

³ using the commercial standard Aircraft Communications Addressing and Reporting System (ACARS, see <http://en.wikipedia.org/wiki/ACARS>), for instance.

status overview as well as useful measurements collected as specific instants (e.g., during engine start). Flight after flight, measurements sent are analyzed in order to detect anomalies that are early signs of degradation. Potential anomalies can be automatically detected by algorithms designed by experts. If an anomaly is confirmed by a human operator, a maintenance recommendation is sent to the company operating the engine.

As a consequence, unscheduled inspections of the engine are sometimes required. These inspections are due to the abnormal measurements. Missing a detection of early signs of degradation can result in an IFSD, an ATO or a delay and cancellation (D&C). Despite the rarity of such events, companies need to avoid them to minimize unexpected expenses and customers' disturbance. Even in cases where an unscheduled inspection does not prevent the availability of the aircraft, it has an attached cost: it is therefore important to avoid as much as possible useless inspections.

We describe in this paper a general methodology to build complex automated decision support algorithms in a way that is comprehensible by human operators who take final decisions. The main idea of our approach is to leverage expert knowledge in order to build hundreds of simple binary indicators that are all signs of the possible existence of an early sign of anomaly in health monitoring data. The most discriminative indicators are selected by a standard forward feature selection algorithm. Then an automatic classifier is built on those features. While the classifier decision is taken using a complex decision rule, the interpretability of the features, their expert based nature and their limited number allows the human operator to at least partially understand how the decision is made. It is a requirement to have a trustworthy decision for the operator.

We will first describe the health monitoring context in Section 2. Then, we will introduce in more details the proposed methodology in Section 3. Section 4 will be dedicated to a simulation study that validates our approach.

2 Context

2.1 Flight data

Engine health monitoring is based in part on flight data acquisition. Engines are equipped with multiple sensors which measure different physical quantities such as the high pressure core speed (N2), the Fuel Metering Valve (FMV), the Exhausted Gas Temperature (EGT), etc. (See Figure 1.) Those measures are monitored in real time during the flight. For instance the quantities mentioned before (N2, FMV, etc.) are analyzed, among others, during the engine starting sequence. This allows one to check the good health of the engine. If potential anomaly is detected, a diagnostic is made. Based on the diagnostic sent to a company operator, the airline may have to postpone the flight or cancel it, depending on the criticality of the fault and the estimated repair time.

The monitoring can also be done flight after flight to detect any change that can be flagged as early signs of degradations. Flight after flight, measurements

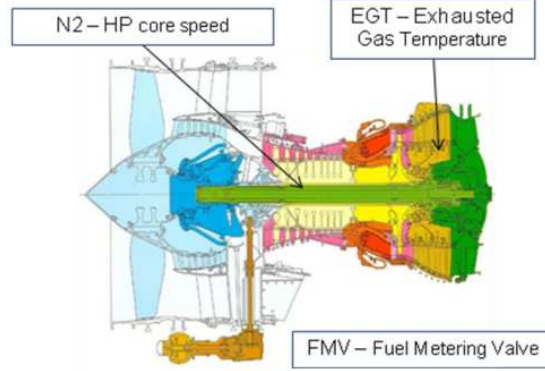


Fig. 1. Localization of some followed parameters on the Engine

are compressed in order to obtain an overview of engines status that consists in useful measurements at specific recurrent moments. These useful measurements are then preprocessed to obtain measurements independent from external environment. These preprocessed data are analyzed by algorithms and human operators. The methodology introduced in this article is mostly designed for this kind of monitoring.

2.2 Detecting faults and abnormal behaviors

Traditional engine health monitoring is strongly based on expert knowledge and field experience (see e.g. [14] for a survey and [5] for a concrete example). Faults and early signs of faults are identified from suitable measurements associated to adapted computational transformation of the data. For instance, the different measurements (temperatures, vibration, etc.) are influenced by the flight parameters (e.g. throttle position) and conditions (outside temperature, etc.). Variations in the measured values can therefore result from variations in the parameters and conditions rather than being due to abnormal behavior. Thus a typical computational transformation consists in preprocessing the measurements in order to remove dependency to the flight context [10].

In practice, the choice of measurements and computational transformations is generally done based on expert knowledge. For instance in [12], a software is designed to record expert decision about a time interval on which to monitor the evolution of such a measurement (or a time instant when such a measurement should be recorded). Based on the recorded examples, the software calibrates a pattern recognition model that can automatically reproduce the time segmentation done by the expert. Once the indicators have been computed, the normal behavior of the indicators can be learned. The residuals between predictions and actual indicators can be statistically modeled, e.g. as a Gaussian vector. A score measurement is obtained from the likelihood of this distribution. The normalized

vector is a failure score signature that may be described easily by experts to identify the fault origin, in particular because the original indicators have some meaning for them. See [4], [5] and [9] for other examples.

However experts are generally specialized on a particular subsystem, thus each algorithm focuses mainly on a specific subsystem despite the need of a diagnostic of the whole system.

2.3 Data and detection fusion

The global diagnostic is currently done by the operator who collects all available results of diagnostic applications. The task of taking a decision based on all incoming information originating from different subsystems is difficult. A first difficulty comes from dependencies between subsystems which means that for instance in some situations, a global early sign of failure could be detected by discovering discrepancies between seemingly perfectly normal subsystems. In addition, subsystem algorithms can provide conflicting results or a decision with a very low confidence level. Furthermore, extreme reliabilities of engines lead to an exacerbated trade off between false alarm levels and detection levels, leading in general to a rather high level of false alarms, at least at the operator level. Finally, the role of the operator is not only to identify a possible early sign of failure, but also to issue recommendations on the type of preventive maintenance needed. In other words, the operator needs to identify the possible cause of the potential failure.

2.4 Objectives

The long term goal of engine health monitoring is to reach automated accurate, trustworthy and precise maintenance decisions during optimally scheduled shop visit, but also to drastically reduce operational events such as IFSD and ATO. However, partly because of the current industrial standard, pure black box modeling is unacceptable. Indeed, operators are currently trained to understand expertly designed indicators and to take complex integrated decisions on their own. In order for a new methodology to be accepted by operators, it has at least to be of a gray box nature, that is to be (partially) explainable via logical and/or probabilistic reasoning. Then, our objective is to design a monitoring methodology that helps the human operator by proposing integrated decisions based on expertly designed indicators with a “proof of decision”.

3 Architecture of the Decision Process

3.1 Health monitoring data

In order to present the proposed methodology, we first describe the data obtained via health monitoring and the associated decision problem.

We focus here on ground based long term engine health monitoring. Each flight produces dozens of timestamped flight events and data. Concatenating those

data produces a multivariate temporal description of an engine whose dimensions are heterogeneous. In addition, sampling rates of individual dimensions might be different, depending on the sensors, the number of critical time points recorded in a flight for said sensor, etc.

Based on expert knowledge, this complex set of time series is turned into a very high dimensional indicator vector. The main idea, outlined in the previous section, is that experts generally know what is the expected behavior of a subsystem of the engine during each phase of the flight. Then the dissimilarity between the expected behavior and the observed one can be quantified leading to one (or several) anomaly scores. Such scores are in turn transformed into binary indicators where 1 means an anomaly is detected and 0 means no anomaly detected.

This transformation has two major advantages: it homogenizes the data and it introduces simple but informative features (each indicator is associated to a precise interpretation related to expert knowledge). It leads also to a loss of information as the raw data are in general non recoverable from the indicators. This is considered here a minor inconvenience as long as the indicators capture all possible failure modes. This will be partially guaranteed by including numerous variants of each indicator (as explained below). On a longer term, our approach has to be coupled with field experience feedback and expert validation of its coverage.

After the expert guided transformation, the monitoring problem becomes a rather standard classification problem: based on the binary indicators, the decision algorithm has to decide whether there is an anomaly in the engine and if, this is the case, to identify the type of the anomaly (for instance by identifying the subsystem responsible for the potential problem).

We describe now in more details the construction of the binary indicators.

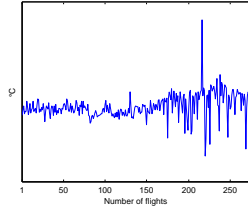
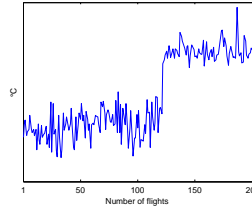
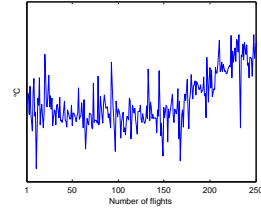
3.2 Some types of anomalies

Some typical univariate early signs of anomalies are shown on Figures 2, 3 and 4 which display the evolution through time of a numerical value extracted from real world data. One can identify, with some practice, a variance shift on Figure 2, a mean shift on Figure 3 and a trend modification (change of slope) on Figure 4. In the three cases, the change instant is roughly at the center of the time window.

The main assumption used by experts in typical situations is that, when external sources of change have been accounted for, the residual signal should be stationary in a statistical sense. That is, observations

$$\mathcal{Y}_n = (Y_1(\theta_1), \dots, Y_n(\theta_n))$$

are assumed to be generated identically and independently from a fixed parametric law, with a constant set of parameters (that is, all the θ_i are identical). Then, detecting an anomaly amounts to detecting a change in the time series (as illustrated by the three Figures above). This can be done via numerous well known statistical tests [1]. In the multivariate cases, similar shifts in the signal

**Fig. 2.** Variance shift**Fig. 3.** Mean shift**Fig. 4.** Trend modification

can be associated to anomalies. More complex scenarios, involving for instance time delays, can also be designed by experts.

3.3 From anomaly types to indicators

While experts can generally describe explicitly what type of change they are expecting for some specific early signs of anomaly, they can seldom provide detailed parameter settings for statistical tests (or even for the aggregation technique that could lead to a statistical test after complex calculations). To maximize coverage it seems natural to include numerous indicators based on variations of the anomaly detectors compatible with expert knowledge.

Let us consider for illustration purpose that the expert recommends to look for shifts in mean of a certain quantity as early signs of a specific anomaly. If the expert believes the quantity to be normally distributed with a fixed variance, then a natural test would be Student's t-test. If the expert has no strong priors on the distribution, a natural test would be the Mann-Whitney U test. Both can be included to maximize coverage.

Then, in both cases, one has to assess the scale of the shift. Indeed those tests work by comparing summary statistics of two populations, before and after a possible change point. To define the populations, the expert has to specify the length of the time windows to consider before and after the possible change point: this is the expected scale at which the shift will appear. In most cases, the experts can only give a rough idea of the scale. Again, maximizing the coverage leads to the inclusion of several scales compatible with the experts' recommendations.

Given the choice of the test, of its scale and of a change point, one can construct a statistic. A possible choice for the indicator could be this value or the associated p -value. However, we choose to use simpler indicators to ease their interpretation. Indeed, the raw value of a statistic is generally difficult to interpret. A p -value is easier to understand because of the uniform scale, but can still lead to misinterpretation by operators with insufficient statistical training. We therefore choose to use binary indicators for which the value 1 corresponds to a rejection of the null hypothesis of the underlying test to a given level (the null hypothesis is here the case with no mean shift).

Finally, as pointed out before, aircraft engines are extremely reliable, a fact that increases the difficulty in balancing sensibility and specificity of anomaly detectors. In order to alleviate this difficulty, we build high level indicators from low level tests. For instance, if we monitor the evolution of a quantity on a long period compared to the expected time scale of anomalies, we can compare the number of times the null hypothesis of a test has been rejected on the long period with the number of times it was not rejected, and turn this into a binary indicator with a majority rule.

To summarize, we construct parametric anomaly scores from expert knowledge, together with acceptable parameter ranges. By exploring those ranges, we generate numerous (possible hundreds of) binary indicators. Each indicator can be linked to an expertly designed score with a specific set of parameters and thus is supposedly easy to interpret by operators. Notice that while we as focused in this presentation on temporal data, this framework can be applied to any data source.

3.4 Decision

The final decision step consists in classifying these high dimensional binary vectors into at least two classes, i.e., the presence or absence of an anomaly. A classification into more classes is highly desirable if possible, for instance to further discriminate between seriousness of anomalies and/or sources (in terms of subsystems of the engine). In this paper however, we will restrict ourselves to a binary classification case (with or without anomaly).

As explained before, we aim in the long term at gray box modeling, so while numerous classification algorithms are available see e.g. [8], we shall focus on interpretable ones. In this paper, we choose to use Random Forests [2] as they are very adapted to binary indicators and to high dimensional data. They are also known to be robust and to provide state-of-the-art classification performances at a very small computational cost. While they are not as interpretable as their ancestors CART [3], they provide at least variable importance measures that can be used to identify the most important indicators.

Finally, while including hundreds of indicators is important to give a broad coverage of the parameter spaces of the expert scores and thus to maximize the probability of detecting anomalies, it seems obvious that some redundancy will appear. Therefore, we have chosen to apply a feature selection technique [6] to this problem. The reduction of number of features will ease the interpretation by limiting the quantity of information transmitted to the operators in case of a detection by the classifier. Among the possible solutions, we choose to use the Mutual information based technique Minimum Redundancy Maximum Relevance (mRMR, [11]) which was reported to give excellent results on high dimensional data.

4 A simulation study

4.1 Introduction

It is difficult to find real data with early signs of degradations, because they are scarce and moreover the scheduled maintenance operations tend to remove these early signs. Experts could study in detail recorded data to find early signs of anomalies whose origins were fixed during maintenance but it is close to looking for a needle in a haystack, especially considering the huge amount of data to analyze. We will therefore rely in this paper on simulated data. Our goal is to validate the interest of the proposed methodology in order to justify investing in the production of carefully labelled real world data.

In this section we begin by the description of the simulated data used for the evaluation of the methodology, and then we will present the performance obtained on this data.

4.2 Simulated data

The simulated data are generated according to the univariate shift models described in Section 3.2. We generate two data sets a simple one A and a more complex one B .

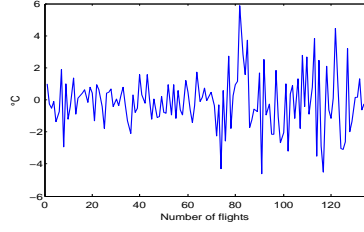
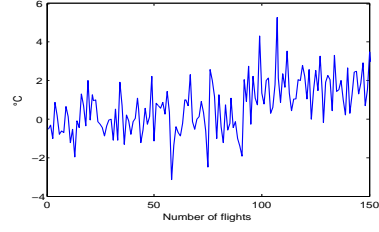
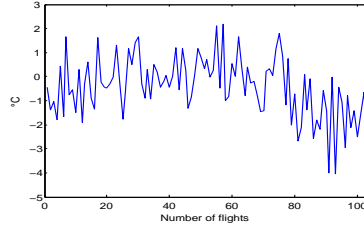
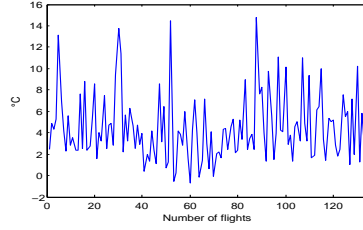
In the first case A , it is assumed that expert based normalisation has been performed. Therefore when no shift in the data distribution occurs, we observe a stationary random noise modeled by the standard Gaussian distribution. Using notations of Section 3.2 the Y_i are independent and identically distributed according to $\mathcal{N}(\mu = 0, \sigma^2 = 1)$. Signals in set A have a length chosen uniformly at random between 100 and 200 observations (each signal has a specific length).

Anomalies are modelled after the three examples given in Figures 2, 3 and 4. We implement therefore three types of shift:

1. a variance shift: in this case, observations are distributed according to $\mathcal{N}(\mu = 0, \sigma^2)$ with $\sigma^2 = 1$ before the change point and σ chosen uniformly at random in $[1.01, 5]$ after the change point (see Figure 5);
2. a mean shift: in this case, observations are distributed according to $\mathcal{N}(\mu, \sigma^2 = 1)$ with $\mu = 0$ before the change point and μ chosen uniformly at random in $[1.01, 5]$ after the change point (see Figure 6);
3. a slope shift: in this case, observations are distributed according to $\mathcal{N}(\mu, \sigma^2 = 1)$ with $\mu = 0$ before the change point and μ increasing linearly from 0 from the change point with a slope chosen uniformly at random in $[0.02, 3]$ (see Figure 7).

Assume that the signal contains n observations, then the change point is chosen uniformly at random between the $\frac{2n}{10}$ -th observation and the $\frac{8n}{10}$ -th observation.

According to this procedure, we generate a balanced data set with 6000 observations corresponding to 3000 observations with no anomaly, and 1000 observations for each of the three types of anomalies.

**Fig. 5.** Variance shift**Fig. 6.** Mean shift**Fig. 7.** Trend modification**Fig. 8.** Data without anomaly but with suboptimal normalisation represented by a slow varying deterministic component

In the second data set, B , a slow deterministic variation is added to randomly chosen signals with no anomaly: this is a way to simulate a suboptimal normalisation (see Figure 8 for an example). The slow variation is implemented by adding to the base noise a sinus with a period of $\frac{2}{3}$ of the signal length and amplitude 1.

Signals in set B are shorter, to make the detection more difficult: they are chosen uniformly at random between 100 and 150 observations. In addition, the noise is modeled by a χ^2 distribution with 4 degrees of freedom. Signals with an anomaly are generated using the same rationale as for set A . In this case however, the mean shift is simply implemented by adding a constant to the signal after the change point. The “variance” shift is in fact a change in the number of degrees of freedom of the χ^2 distribution: after the change point, the number of degrees is chosen randomly (uniformly) between 8 and 16. The change point is chosen as in set A .

According to this procedure, we generate a balanced data set with 6000 observations corresponding to 3000 observations with no anomaly, and 1000 observations for each of the three types of anomalies. Among the 3000 anomaly free signals, 1200 are corrupted by a slow variation.

4.3 Indicators

As explained in Section 3.3, binary indicators are constructed from expert knowledge by varying parameters, including scale and position parameters. In the

present context, we use sliding windows: for each position of the window, a classical statistical test is conducted to decide whether a shift in the signal occurs at the center of the window.

The “expert” designed tests are here:

1. the Mann–Whitney–Wilcoxon U test (non parametric test for shift in mean);
2. the two sample Kolmogorov-Smirnov test (non parametric test for differences in distributions);
3. the F-test for equality of variance (parametric test based on a Gaussian hypothesis).

The direct parameters of those tests are the size of the window which defines the two samples (30, 50, and $\min(n - 2, 100)$ where n is the signal length) and the level of significance of the test (0.005, 0.1 and 0.5). Notice that those tests do not include a slope shift detection.

Then, more complex binary indicators are generated, as explained in Section 3.3. In a way, this corresponds to build very simple binary classifiers. We use the following ones:

1. for each underlying test, the derived binary indicator takes the value one if on a fraction β of m windows, the test detects a change. Parameters are the test itself with its parameters, the value of β (we considered 0.1, 0.3 and 0.5) and the number of observations in common between two consecutive windows (the length of the window minus 1, 5 or 10);
2. for each underlying test, the derived binary indicator takes the value one if on a fraction β of m consecutive windows, the test detects a change (same parameters);
3. for each underlying test, the derived binary indicator takes the value one if there are 5 consecutive windows such that the test detects a change on at least k of these 5 consecutive windows (similar parameters where β is replaced by k).

In addition, based on expert recommendation, we apply all those indicators both to the original signal and to a smoothed signal (using a simple moving average over 5 measurements).

We use more than 50 different configurations for each indicator, leading to a total number of 810 binary indicators (it should be noted that only a subset of all possible configurations is included into this indicator vector).

4.4 Reference performances

In this paper, we focus on the simple case of learning to discriminate between a stationary signal and a signal with a shift. We report therefore the classification rate (classification accuracy).

For both sets A et B , the learning sample is composed of 1000 signals keeping the balance between the three classes of shifts. The evaluation is done on the remaining 5000 signals that have been divided in 10 groups of 500 time series

each. The rationale of this data splitting in the evaluation phase is to estimate both the prediction quality of the model but also the variability in this rate as an indication of the trust we can put on the results. We also use and report the out-of-bag (OOB) estimate of the performances provided by the Random Forest (this is a byproduct of the bootstrap procedure used to construct the forest, see [2]).

When all the 810 indicators are used, the classification performances are very high on set *A* and acceptable on set *B* (see Table 1). The similarity between the OOB estimate of the performances and the actual performances confirms that the OOB performances can be trusted as a reliable estimator of the actual performances. Data set *B* shows a strong over fitting of the Random Forest, whereas data set *A* exhibits a mild one.

Data set	Training set accuracy	OOB accuracy	Test set average accuracy
<i>A</i>	1	0.953	0.957 (0.0089)
<i>B</i>	1	0.828	0.801 (0.032)

Table 1. Classification accuracy of the Random Forest using the 810 binary indicators. For the test set, we report the average classification accuracy and its standard deviation between parenthesis.

4.5 Feature selection

On the data set *A*, the performances are very satisfactory, but the model is close to a black box in the sense that it uses all the 810 indicators. Random Forests are generally difficult to interpret, but a reduction in the number of indicators would allow an operator to study the individual decisions performed by those indicators in order to have a rough idea on how the global decision could have been made. On the data *B* set, the strong over fitting is another argument for reducing the number of features.

Using the mRMR we ranked the 810 indicators according to a mutual information based estimation of their predictive performances. We use then a forward approach to evaluate how many indicators are needed to achieve acceptable predictive performances. Notice that in the forward approach, indicators are added in the order given by mRMR and then never removed. As mRMR takes into account redundancy between the indicators, this should not be a major issue. Then for each number of indicators, we learn a Random Forest on the learning set and evaluate it.

Figure 9 shows the results for data set *A*. Accuracies are quite high with a rather low number of indicators, with a constant increase in performances on the learning set (as expected) and a stabilisation of the real performances (as evaluated by the test set and the OOB estimation) around roughly 40 indicators.

Figure 10 shows the results for data set *B*. Excepted the lower performances and the stronger over fitting, the general behavior is similar to the case of data set

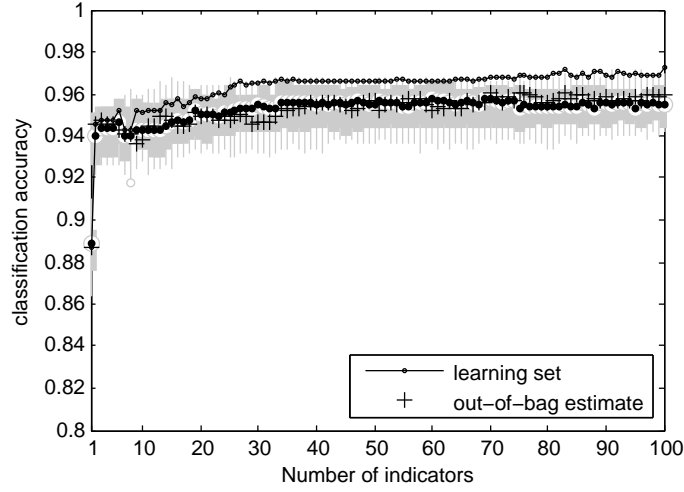


Fig. 9. Data set A : classification accuracy on learning set (circle) as a function of the number of indicators. A boxplot gives the classification accuracies on the test subsets, summarized by its median (black dot inside a white circle). The estimation of those accuracies by the out-of-bag (OOB) bootstrap estimate is shown by the crosses.

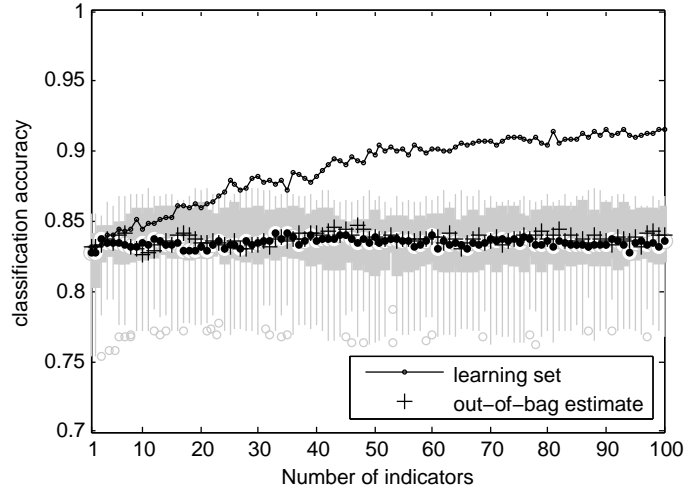


Fig. 10. Data set B : classification accuracy on learning set (circle) as a function of the number of indicators. A boxplot gives the classification accuracies on the test subsets, summarized by its median (black dot inside a white circle). The estimation of those accuracies by the out-of-bag (OOB) bootstrap estimate is shown by the crosses.

A. Those lower performances were expected because data set B has been designed to be more difficult to analyze, in part because of the inadequacy between the actual data model (χ^2 distribution) and the “expert” based low level tests (in particular the F test which assumes Gaussian distributions).

In both cases, the feature selection procedure shows that only a small subset of the original 810 indicators is needed to achieve the best performances reachable on the data sets. This is very satisfactory as this allows to present to operators a manageable number of binary decisions together with the aggregated one provided by the random forest.

4.6 Selected indicators

In order to illustrate further the interest of the proposed methodology, we show in Table 2 the best ten indicators for data set A . Those indicators lead to quite good performances with an average test set classification accuracy of 0.944 (OOB estimation is 0.938).

type of indicator	level	window length	window step
F test	0.005	100	5
confu(2,3)	0.005	50	5
ratef(0.1)	0.005	50	5
KS test	0.005	100	1
conff(3,5)	0.005	100	5
KS test	0.1	100	5
F test	0.005	100	1
KS test	0.005	100	10
lseqf(0.1)	0.1	50	1
F test	0.005	50	10

Table 2. The best ten indicators according to mRMR for data set A . Confu(k,n) corresponds to a positive Mann–Whitney–Wilcoxon U test on k windows out of n consecutive ones. Conff(k,n) is the same thing for the F-test. Ratef(α) corresponds to a positive F-test on $\alpha \times m$ windows out of m . Lseqf(α) corresponds to a positive F-test on $\alpha \times m$ consecutive windows out of m . Lsequ(α) is the same for a U test. Here, none of the indicators are based on a smoothed version of the signal.

Table 3 shows the best ten indicators for data set B . Again, this corresponds to quite good performances with an average test set classification accuracy of 0.831 (OOB estimation is 0.826). As expected, the F test and indicators based on it are less interesting for this data set as the noise is no more Gaussian.

In both cases, we see that the feature selection method is able to make a complex selection in a very large set of binary indicators. This induces indirectly an automatic tuning of the parameters of the low level tests and of simple aggregation classifiers. Because of their simplicity and their binary outputs, indicators are easy to understand by an operator.

type of indicator	level	window length	smoothed	window step
KS test	0.005	100	no	5
lseqf(0.1)	0.1	30	yes	1
confu(4,5)	0.005	30	no	1
U test	0.1	100	no	5
confu(4,5)	0.005	100	no	5
confu(2,3)	0.005	100	no	1
lsequ(0.3)	0.1	50	no	1
F test	0.005	100	yes	10
confu(2,3)	0.005	30	no	5
KS Test	0.005	100	no	10

Table 3. The best ten indicators according to mRMR for data set B . Please refer Table 2 for notations.

5 Conclusion and perspectives

In this paper, we have introduced a diagnostic methodology for engine health monitoring that leverage expert knowledge and automatic classification. The main idea is to build from expert knowledge parametric anomaly scores associated to range of plausible parameters. From those scores, hundreds of binary indicators are generated in a way that covers the parameter space as well as introduces simple aggregation based classifiers. This turns the diagnostic problem into a classification problem with a very high number of binary features. Using a feature selection technique, one can reduce the number of useful indicators to a humanly manageable number. This allows a human operator to understand at least partially how a decision is reached by an automatic classifier. This is favored by the choice of the indicators which are based on expert knowledge and on very simple decision rules. A very interesting byproduct of the methodology is that it can work on very different original data as long as expert decision can be modelled by a set of parametric anomaly scores. This was illustrated by working on signals of different lengths.

Using simulated data, we have shown that the methodology is sound: it reaches good predictive performances even with a limited number of indicators (e.g., 10). In addition, the selection process behaves as expected, for instance by discarding statistical tests that are based on hypothesis not fulfilled by the data. However, we limited ourselves to univariate data and to a binary classification setting (i.e., abnormal versus normal signal). We need to show that the obtained results can be extended to multivariate data and to complex classification settings (as identifying the cause of a possible anomaly is extremely important in practice).

It should also be noted that we relied on Random Forests which are not as easy to interpret as other classifiers (such as CART). In our future work, we will compare Random Forest to simpler classifiers. As we are using binary indicators, some form of majority voting is probably the simplest possible rule but using such as rule implies to choose very carefully the indicators [13].

Finally, it is important to notice that the classification accuracy is not the best way of evaluating the performances of a classifier in the health monitoring context. Firstly, health monitoring intrinsically involves a strong class imbalance [7]. Secondly, health monitoring is a cost sensitive area because of the strong impact on airline profit of an unscheduled maintenance. It is therefore important to take into account specific asymmetric misclassification cost to get a proper performance evaluation.

References

1. Basseville, M., Nikiforov, I.V.: Detection of abrupt changes: theory and applications. *Journal of the Royal Statistical Society-Series A Statistics in Society* 158(1), 185 (1995)
2. Breiman, L.: Random forests. *Machine learning* 45(1), 5–32 (2001)
3. Breiman, L., Friedman, J.H., Olshen, R.A., Stone, C.J.: *Classification and regression trees*. wadsworth & brooks. Monterey, CA (1984)
4. Côme, E., Cottrell, M., Verleysen, M., Lacaille, J.: Aircraft engine health monitoring using self-organizing maps. In: *Advances in Data Mining. Applications and Theoretical Aspects*, pp. 405–417. Springer (2010)
5. Flandrois, X., Lacaille, J., Masse, J.R., Ausloos, A.: Expertise transfer and automatic failure classification for the engine start capability system. *AIAA Infotech*, Seattle, WA (2009)
6. Guyon, I., Elisseeff, A.: An introduction to variable and feature selection. *The Journal of Machine Learning Research* 3, 1157–1182 (2003)
7. Japkowicz, N., Stephen, S.: The class imbalance problem: A systematic study. *Intelligent data analysis* 6(5), 429–449 (2002)
8. Kotsiantis, S.B., Zaharakis, I., Pintelas, P.: Supervised machine learning: A review of classification techniques (2007)
9. Lacaille, J.: A maturation environment to develop and manage health monitoring algorithms. PHM, San Diego, CA (2009)
10. Lacaille, J.: Standardized failure signature for a turbofan engine. In: *Aerospace conference*, 2009 IEEE. pp. 1–8. IEEE (2009)
11. Peng, H., Long, F., Ding, C.: Feature selection based on mutual information criteria of max-dependency, max-relevance, and min-redundancy. *Pattern Analysis and Machine Intelligence, IEEE Transactions on* 27(8), 1226–1238 (2005)
12. Rabenoro, T., Lacaille, J.: Instants extraction for aircraft engine monitoring. *AIAA Infotech@Aerospace* (2013)
13. Ruta, D., Gabrys, B.: Classifier selection for majority voting. *Information fusion* 6(1), 63–81 (2005)
14. Tumer, I.Y., Bajwa, A.: A survey of aircraft engine health monitoring systems. In: *Proc. 35th Joint Propulsion Conf* (1999)
15. Vasov, L., Stojiljković, B.: Reliability levels estimation of JT8D-9 and CFM56-3 turbojet engines. *FME Transactions* 35(1), 41–45 (2007)